World Research Journal of Applied Physics
ISSN: 0976-7673 & E-ISSN: 0976-7681, Vol. 1, Issue 1, 2010, pp-05-13.
Available online at http://www.bioinfo.in/contents.php?id=52

INFLUENCE OF SINTERING AIDS ON STRUCTURAL CHARACTERISTICS OF $(Ba_{1-x}Gd_x)TiO_3$

GAMA S.B. AND RAIBAGKAR R.L.*
Department of Post Graduate Studies and Research in Materials Science, Gulbarga University, Gulbarga-585106 (Karnataka) India.
*Corresponding Author: Email- rlraibagkar@rediffmail.com

Abstract- The ferroelectric ceramic samples with composition $(Ba_{1-x}Gd_x)TiO_3$ (x=0.001, 0.002, 0.004 and 0.005) with YST(1 mol% Y_2O_3, 7.5 mol% SiO_2 and 3 mol% of excess TiO_2) (SBGT) were prepared by employing a solid-state reaction technique. XRD patterns of the well sintered powders revealed the tetragonal structure at room temperature. The variation in the lattice parameters is non-linear, provides an evidence for B-site substitution. Micro-structural data of the synthesized samples were studied by scanning electron microscope. Compositional study was carried out using energy dispersive analysis by X-rays. It was observed that the Gd-substitution significantly reduces the grain size with a tendency of agglomeration.

1. INTRODUCTION

Barium titanate is one of the best known perovskite ferroelectric compounds ($A^{2+}B^{4+}O_3$) that have been extensively studied [1] due to simplicity of crystal structure, which can accommodate different types of dopant. The electrical properties of $BaTiO_3$ depend strongly on its microstructure as well as its chemical composition. The electrical resistivity and the relative permittivity at Curie temperature of $BaTiO_3$ are all affected by its microstructure [2] at high temperature, the rare-earth elements dissolve in both the A-and B-sites, depending on the A/B ratio in $BaTiO_3$. Hiroshi Kishi et al [3] reported that rare earth elements are believed to act as a donor in the Ba-site or as an acceptor when they dissolve in the Ti-site. Aliovalent dopants have a profound influence on micro-structural developments and the resultant electrical properties of $BaTiO_3$-based ceramics [4]. Thus, the microstructure of $BaTiO_3$ can be controlled by two approaches, either by additives, to effectively prevent discontinuous grain growth or novel method of preparation to tailor the microstructure [5].

Normally, donor-doped $BaTiO_3$ ceramics can be prepared by the mixed oxides solid state reaction method. SiO_2 or a eutectic mixture like Al_2O_3-SiO_2-TiO_2 (AST) or Y_2O_3-SiO_2-TiO_2 (YST) is added as the sintering aids, which results in the formation of liquid phase at 1260-1240^{0}C, thereby lowering the sintering temperature [6]. Usually, the microstructure of such ceramics is a result of liquid phase sintering. The required liquid phase is formed by a reaction between a suitable additive and the $BaTiO_3$ matrix powder. Addition of SiO_2 can promote anomalous grain growth and lower the sintering temperature of $BaTiO_3$ ceramics. Chen et al [7] studied the effect of YST

sintering aids on microstructure and electrical properties of $(Pb_{0.6}Sr_{0.3}Ba_{0.1})TiO_3$ revealed incorporation of sintering aids. SiO_2 has lowered the sintering temperature necessary from 1250^oC (10 min) to 1140^oC (10 min) by employing microwave sintering. The materials were stabilized only when they contained more than 7.5mol% SiO_2 and were sintered at 1120^oC (10 min) and higher temperature. Here, study is being carried out to investigate the effect of additives on the structure of Gd-doped $BaTiO_3$ sintered at lower temperature, i.e., 1120^0C.

2. EXPERIMENTAL PROCEDURE

The ceramic sample having composition $(Ba_{1-x}Gd_x)TiO_3$ (SBGT) with x=0.001-0.005 were prepared by solid-state reaction method. High purity (99.99%) chemicals, $BaCO_3$, TiO_2, Gd_2O_3, $Y2O_3$ and SiO_2 in their stoichiometric proportions SBGT samples were labeled as $SBGT_1$ for x=0.001, $SBGT_2$ for x=0.002, $SBGT_3$ for x=0.004, and $SBGT_4$ for x=0.005 with sintering aids YST (1 mol% Y_2O_3, 7.5 mol% SiO_2 and 3 mol% of excess TiO_2) were weighed, mixed and grounded thoroughly in an agate mortar for 4 hrs. SBGT samples were calcined in air media at 950^0C and at 1000^0C for 8 hrs in alumina crucibles, with intermediate grindings for 2 hrs, in a programmable high temperature muffle furnace. The finished powder was pressed into circularly shaped disc pellets of 10mm diameter and thickness of 1.5 mm using tungsten carbide dye and plunger with hydrostatic pressure of $45kN/m^2$ using aqueous (5%) polyvinyl alcohol. Pellets were sintered at 1120^0C and annealed at 1050^0C for 1hr respectively. The heating and cooling rate for all thermal cycles was 2^0C/min.

X-ray diffractograms of the samples were obtained by employing X-ray diffractometer (Phillips PRO PANalytical, UK) with CuK_α radiations (λ=1.54056Å) and Ni-filter, operated at 40kV and 30mA, in a continuous scanning mode. 2θ-range was 10^0-80^0, with step-size of 0.017^0. The microstructure and the compositional distribution were examined using scanning electron microscope (SEM) attached with energy dispersive analysis of X-rays (EDAX) (model JSM-8048/SM JEOL-Japan).

3. RESULTS AND DISCUSSION

Room temperature x-ray diffraction profiles of SBGT samples are displayed in Figure 1. Analyses of XRD patterns suggest that phase composition was tetragonal. Sharp and single peak indicate good homogeneity and formation of single-phase compound. X-ray diffraction data of the SBGT samples have been indexed on the basis tetragonal structure of $BaTiO_3$. Table 1 lists the least squares fitting method derived lattice parameters, tetragonality (i.e., c/a) ratio and the lattice volume of the samples. It is observed that, lattice parameters, c and a changes with Gd concentration (x), which reveals that the incorporation of Gd affects the crystal lattice of $BaTiO_3$. Since the ionic radius of Gd^{3+} is larger than Ti^{4+} (=0.68Å), there is reduction in c-axis and simultaneous slight extension in the a-axis for $SBGT_1$ and $SBGT_2$ where as in samples $SBGT_3$ and $SBGT_4$, there is a slight increase in c-axis and decrease in a-axis. Also, change in lattice parameters suggests that this substitution takes place in both A- and B-sites of the perovskite as evidenced by Bo Li et al [8]. As evident from X-ray diffraction patterns, there is a small shift in peaks towards the higher 2θ-angle except in BGT_1. As x is increased, the (c/a) ratio decreases with the x for $SBGT_1$ and $SBGT_2$, whereas for $SBGT_3$ and $SBGT_4$ it increases. This decrease in (c/a) can be attributed to the cationic size effect. When Gd^{3+} enters into the crystal lattice, it occupies the Ba-site at lower substitution content.

XRD profiles focusing on the prominent <111>, <002> and <200> peaks are shown in Fig. 2. It confirms the formation of single-phase and tetragonal crystal structure. The <002> and <200> peak profile for each sample is shown in Table 2. (c/a)-ratio decreases gradually, corresponding to the change in <002> and <200> diffraction peaks. The unit cell volume increases with increase in $SBGT_2$.

The average density (ρ) for SBGT samples have been calculated from the molecular weight and volume of the unit cell and are found to be 6.0503 gm/cm^3. The particle size (P) of the sample was calculated from the strongest peak using Scherrer's equation [9],

$P = K\lambda/(B_{1/2} \cos\theta_B)$ - - - - - (3)

where K is constant (0.89) and $B_{1/2}$ is full width half maximum, λ is wavelength of X- rays used and θ is Bragg angle. The particle size of the compound was found to be in the range of 54 to 81nm.

Kreuer[10] reported about the Goldschmidt's relation between stability of the perovskite-type protonic conductors and tolerance factor

$t = (R_A+R_B)/(R_B+R_O)\sqrt{2}$ - - - - (4)

where R_A, R_B, and R_O are the average ionic radii of A- and B-site ions the O-ion respectively. Table 1 lists the tolerance factor (t), x-ray density (ρ) and particle size (P) of all the sintered samples.

Figure 3 shows a distinguishable microstructure with bi-modal grain size distribution in SBGT ceramics. The samples having heterogeneous grains are having grain sizes in the range of 110 nm-200 nm and 0.5-1.5μm. It is evident that, the size of the particles increases with the Gd-content.

The compositional characterization of SBGT powder sample was carried out using EDAX-compositional pattern. The EDAX detector measures the number of emitted X-rays versus their energy. The energy of X-ray is characteristic of element from which the X-ray was emitted. A spectrum of energy versus relative counts of the detected x-rays is obtained and evaluated their qualitative and quantitative determinations of the elements present in the sample volume. An exemplary EDAX pattern for $SBGT_3$ ceramic sample is shown in figure 4. It can be seen from figure 4 that, the constituents within the compound are without any loss, either during processing or sintering of $SBGT_3$. The small deviation from the calculated composition could be due to the loss of oxygen during the sintering of these compounds at high temperatures. The high sintering temperature could easily results in to deficiency of oxygen. Also, charge compensation mechanism involved due to the trivalent rare earth ions substitution could contribute to the creation of oxygen vacancies.

4. CONCLUSIONS

The inclusion of sintering aids lowered the sintering temperature. The room temperature structure of Gd-doped $BaTiO_3$ is tetragonal. The variation in the lattice parameters is non-linear, provides an evidence for B-site substitution. The decrease in (c/a) ratio is not monotonic but strongly depends on x. SBGT samples has a bi-modal grain size distribution, i.e., < 0.1μm and also particles size of >1μm.

ACKNOWLEDGEMENTS

One of the authors (GSB) would like to thank University Grants Commission, New Delhi, India for the award of Teacher Fellowship.

REFERENCES

[1]. F. F, Hammad, A. K. Mohamed and A. M. El-Shabiny, Egypt. J. Solids., 31(1) (2008) 55.

[2]. W. H. Tzing, W. H. Tuan and H. L. Lin, Ceramic International, 25 (1999) 425.

[3]. Hiroshi Kishi, Youichi Mizuno and Hirokazu Chazono, Jap. J. Appl. Phys., 42 (2003) 1.

[4]. L. A.Xue, Y. Chen and R. J. Brook, Mat Sci. Engg., B. 1 (1988) 193.
[5]. Hyun Tae Kim, and Young Ho. Han, Ceramic International, 30 (2004) 1219
[6]. Wang X. X. Chan H. L. W. Pang G. K. H. and Choy, Mat. Sci. Engg. B., 100, (2003) 286.
[7]. Chen Ti. Hu, Hong-Wen Chen, Hong-Yi Chen and I-Nan Lin, Jpn. J. Appl. Phys., 37 (1998) 186.
[8]. Bo Li, Shuren Zang and Xiaohua Zou., J. Mat. Sci. 42 (2007) 5223.
[9]. R. J. Villy, S. A. Oliveri, G. Oliveri and G. Busca, J. Mater. Res., 8(6)(1993) 1418.
[10]. K. D. Kreuer, Sol. St. Ionics, 97 (1997) 1.

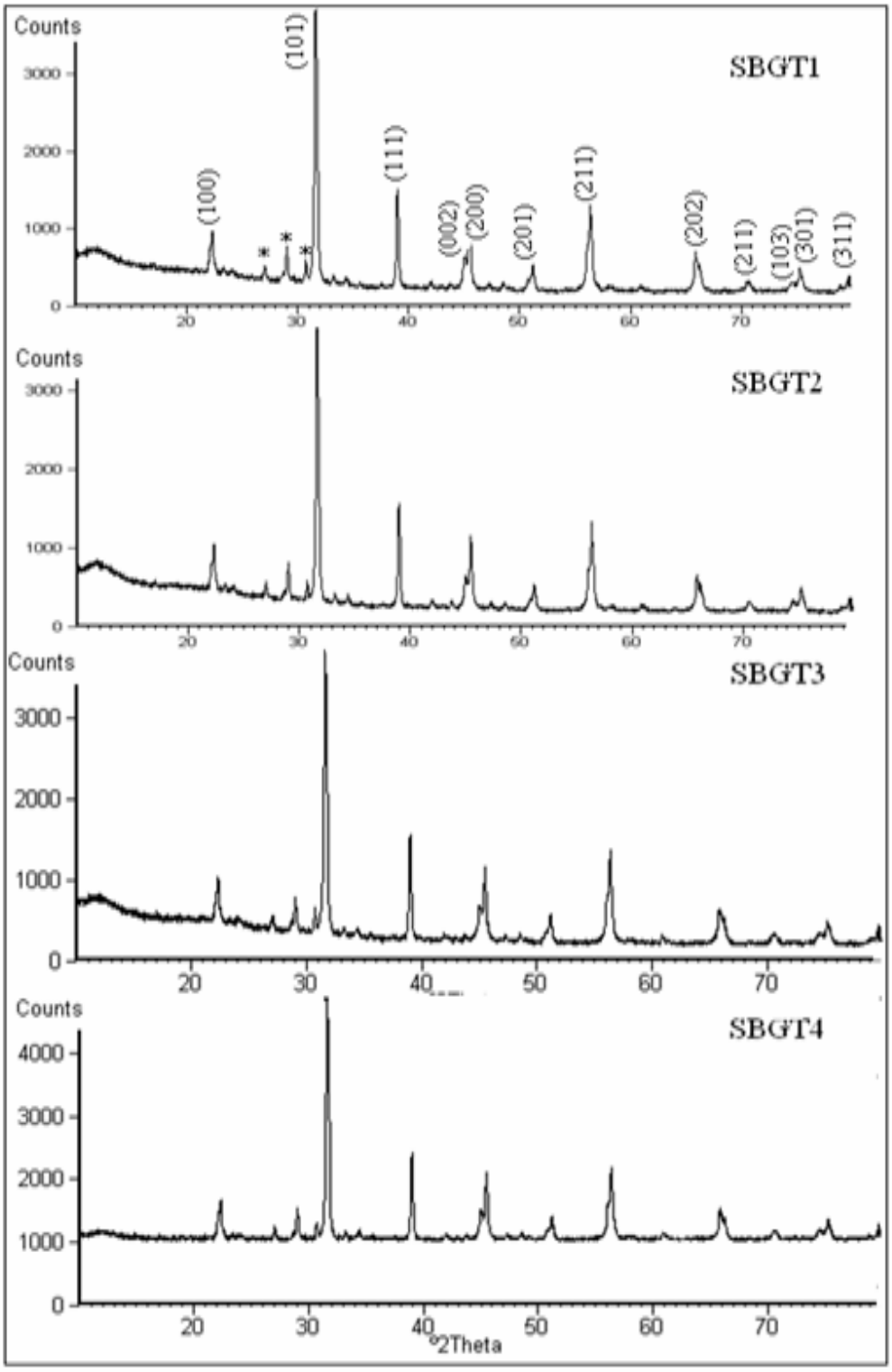

8*

Fig. 1- XRD patterns of synthesized SBGT samples (* shows the reflections due to YST)

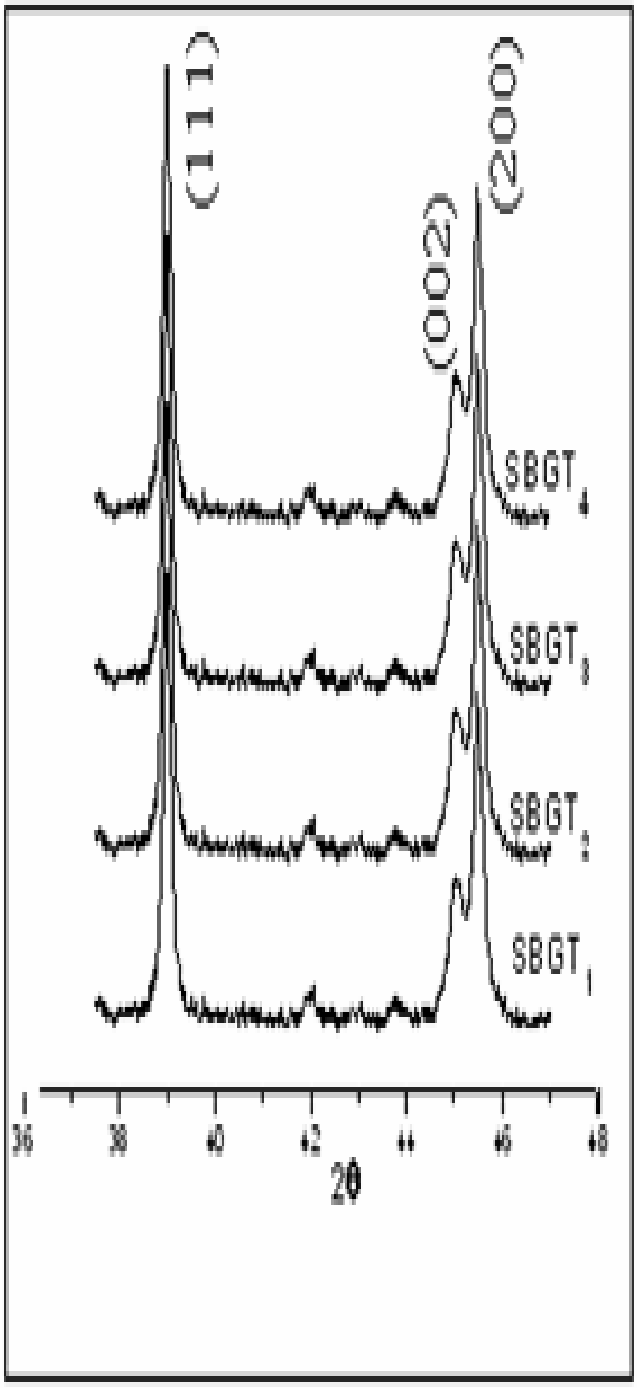

Fig. 2- XRD profile of (111), (002) and (200) peaks of SBGT samples

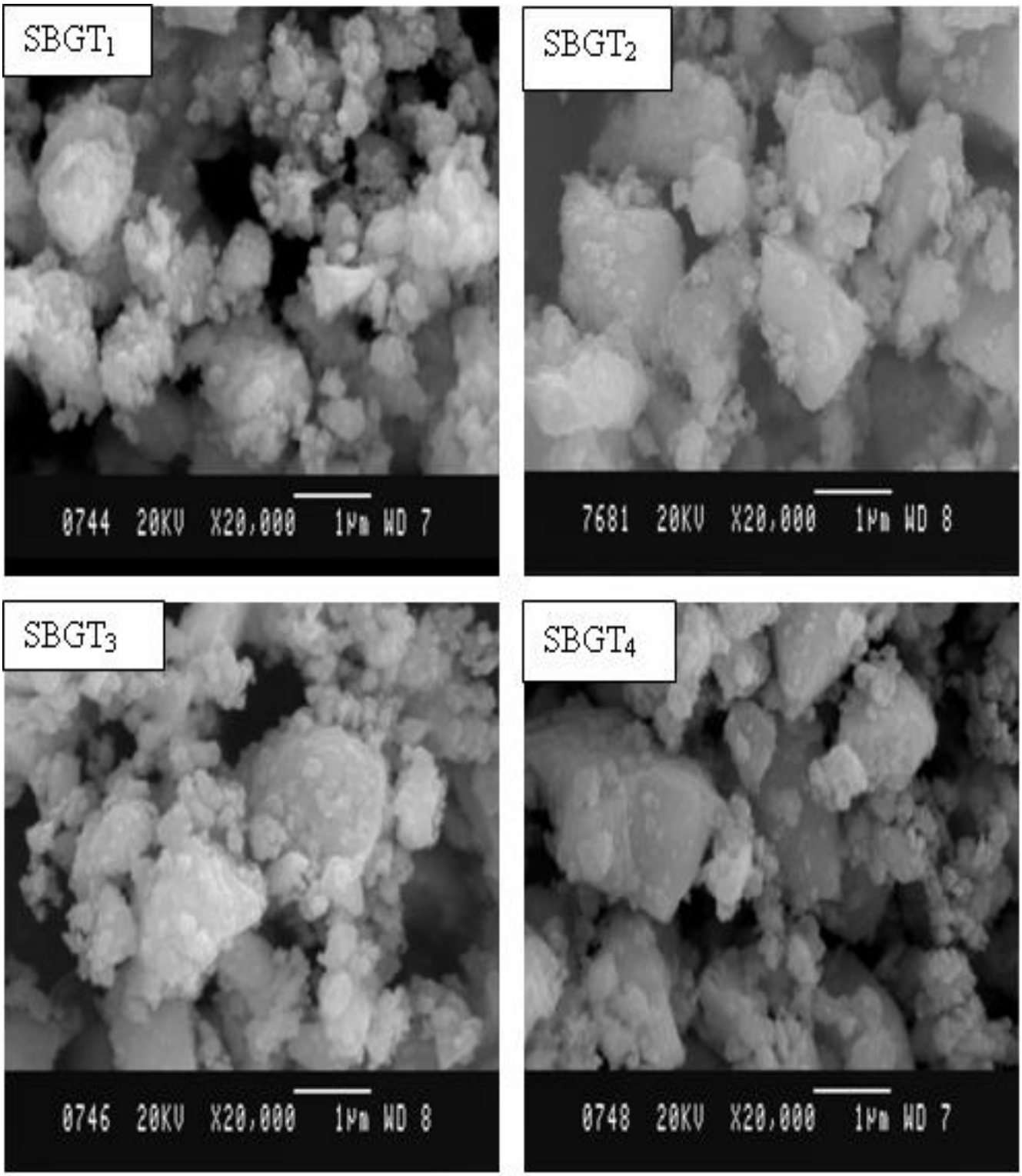

Fig. 3- SEM images for SBGT samples

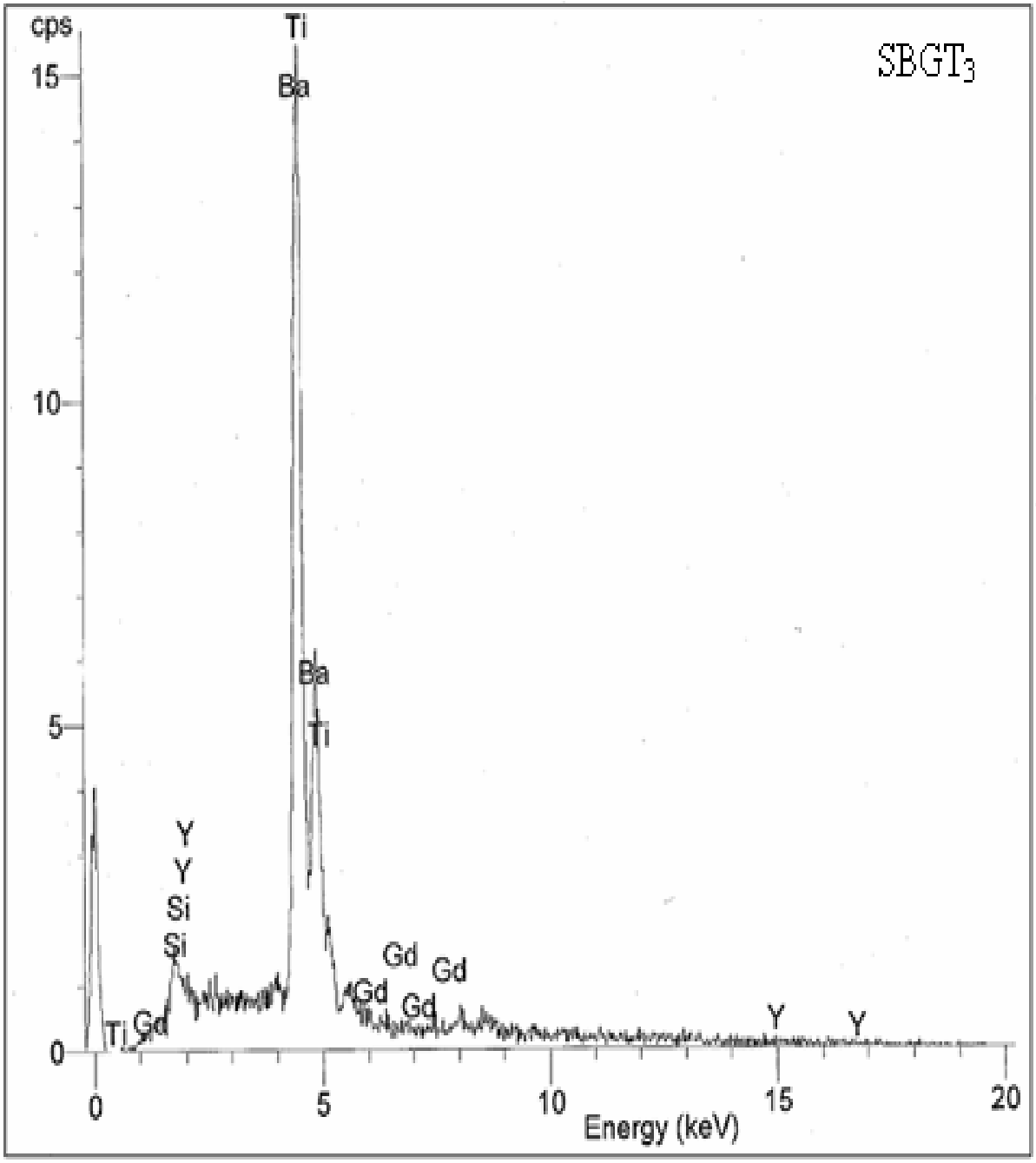

Fig. 4- EDAX spectra for $SBGT_3$

Table 1- Structural data of synthesized samples

Sample code	Tolerance factor (t)	Lattice parameters (Å)		Tetragonality ratio	X-ray Density (gm/cm^3)	Volume $(A^0)^3$	Particle size (nm)
		c	a	(c/a)	ρ	V	P
$SBGT_1$	0.952	4.0266	3.9856	1.0103	6.053886	63.9634	60.9928
$SBGT_2$	0.9581	4.0233	3.9916	1.0079	6.050874	64.0007	81.3216
$SBGT_3$	0.9578	4.0283	3.9859	1.0106	6.052200	63.9976	60.9928
$SBGT_4$	0.9576	4.0299	3.9846	1.0114	6.054014	63.9839	54.2052

Table 2- 2θ and intensity for xrd peaks

Peaks →	(111)		(002)		(200)	
Sample code↓	2θ (°)	I (arb. Units)	2θ (°)	I (arb. Units)	2θ (°)	I (arb. Units)
SBGT1	38.989	1540	45.09	627	45.46	1121
$SBGT_2$	38.989	1507	44.99	622	45.46	1131
$SBGT_3$	38.989	1507	44.99	637	45.46	1123
$SBGT_4$	38.989	1589	45.04	677	45.483	1267